Vision Research 91 (2013) 108–117

Contents lists available at ScienceDirect

Vision Research

journal homepage: www.elsevier.com/locate/visres

Pooling of first-order inputs in second-order vision

Zachary M. Westrick [a,*], Michael S. Landy [a,b]

[a] Department of Psychology, New York University, USA
[b] Center for Neural Science, New York University, USA

ARTICLE INFO

Article history:
Received 7 May 2013
Received in revised form 22 July 2013
Available online 27 August 2013

Keywords:
Second-order vision
Texture

ABSTRACT

The processing of texture patterns has been characterized by a model that first filters the image to isolate one texture component, then applies a rectifying nonlinearity that converts texture variation into intensity variation, and finally processes the resulting pattern with mechanisms similar to those used in processing luminance-defined images (spatial-frequency- and orientation-tuned filters). This model, known as FRF for filter rectify filter, has the appeal of explaining sensitivity to second-order patterns in terms of mechanisms known to exist for processing first-order patterns. This model implies an unexpected interaction between the first and second stages of filtering; if the first-stage filter consists of narrowband mechanisms tuned to detect the carrier texture, then sensitivity to high-frequency texture modulations should be much lower than is observed in humans. We propose that the human visual system must pool over first-order channels tuned to a wide range of spatial frequencies and orientations to achieve texture demodulation, and provide psychophysical evidence for pooling in a cross-carrier adaptation experiment and in an experiment that measures modulation contrast sensitivity at very low first-order contrast.

1. Introduction

Early visual processing has been successfully characterized in terms of linear filtering. In such models, images are analyzed by largely independent channels that are orientation-selective and tuned for spatial and temporal frequency. Linear filters are unhelpful, however, in detecting patterns formed by variation in texture. These patterns, termed second-order images, are visually salient but cannot be detected by purely linear mechanisms if they have nearly uniform mean intensity at the scale of the texture-defined pattern. The Filter Rectify Filter (FRF) model (Fig. 1) has been proposed as a mechanism for processing second-order images. Under FRF, the image is first analyzed by linear filters matched to one of the image's constituent textures, producing areas of high variance but zero mean wherever that texture was present. These responses are then rectified, resulting in higher average response wherever that texture was located. After rectification, texture images can be processed via multiple linear spatial frequency channels, just as luminance images are. Thus, with some preprocessing, the visual system can use similar mechanisms to process scenes defined by texture and scenes defined by light and dark.

This paper is concerned with the properties of the first-stage filter. Specifically we ask: is the first-stage filter a single psychophysical channel? Second-order images are typically constructed from one or more carriers, each varying spatially in contrast or other local parameter (e.g., local orientation or spatial frequency). Several studies have directly addressed whether cortical filtering occurs before or after the nonlinearity in second-order processing by attempting, and failing, to describe human performance with an early nonlinearity (Dakin & Mareschal, 2000; Graham, 1994; Scott-Samuel & Georgeson, 1999). The ability of subjects to detect modulation in orientation (Kingdom & Keeble, 1999; Kingdom, Keeble, & Moulden, 1995; Landy & Oruç, 2002; Larsson, Landy, & Heeger, 2006; Motoyoshi & Nishida, 2004; Prins & Kingdom, 2006) and spatial frequency (Prins & Kingdom, 2002, 2006) demonstrates that first-stage filtering must be selective for both orientation and spatial frequency. Evidence for scale invariance (Kingdom & Keeble, 1999) suggests that early and late filters are matched to the carrier and modulator respectively. This has led to the appealingly simple idea that second-order patterns are detected by second-stage filters matched to the modulator that get as input the rectified responses of first-stage filters matched to the carrier. These first-stage filters are often modelled as typical psychophysical channels as implemented by V1 simple cells with frequency bandwidth of around one octave and orientation bandwidth of around 30° (Landy & Oruç, 2002; Motoyoshi & Nishida, 2004; Prins & Kingdom, 2006).

Several studies have challenged the notion that first-stage filtering is carried out by a single carrier-matched first-order channel. Motoyoshi and Nishida (2004) demonstrated summation between orthogonal carriers in micropattern textures, while Graham, Sutter, and Venkatesan (1993) estimated the bandwidth

* Corresponding author. Address: New York University, Department of Psychology, 6 Washington Place, Rm. 957, New York, NY 10003, USA.
E-mail address: zackwestrick@nyu.edu (Z.M. Westrick).

0042-6989/$ - see front matter © 2013 Elsevier Ltd. All rights reserved.
http://dx.doi.org/10.1016/j.visres.2013.08.005

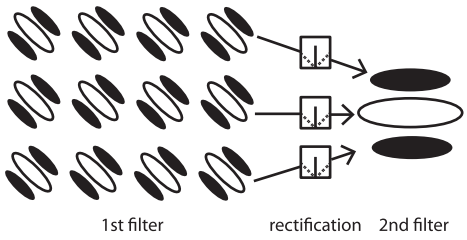

Fig. 1. Schematic FRF model. The first stage consists of a bank of linear filters selective for one of the image's carrier textures. Their responses are then rectified, creating a texture-intensity image. Finally, this texture-intensity image is processed by typical spatial-frequency- and orientation-tuned linear filters to detect any texture modulation.

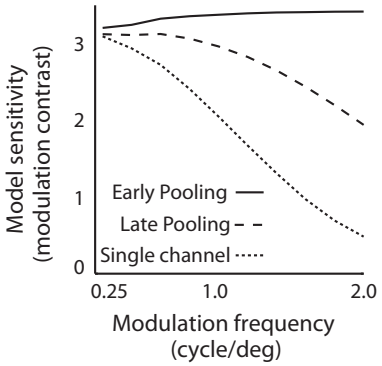

Fig. 3. Predicted contrast sensitivity functions for three models of second-order processing: a single-channel FRF model, pooling before rectification and pooling after rectification.

of first-stage filters used in a texture segregation task to be about twice the bandwidth of standard first-order channels. Using first-order adaptation and a second-order discrimination task, Prins and Kingdom (2002) showed, for textures defined by orientation or frequency modulation, that the early filters used in the task are tuned off-frequency and off-orientation from the carrier, and that this off-carrier tuning maximizes sensitivity to the modulation. These studies suggest that the visual system has some flexibility in selecting first-order inputs to second-order mechanisms when the structure of the stimuli and task demands it. We will demonstrate that even with stimuli that do not appear to favor broadband or off-carrier tuned first-order filters, such as sinusoidal modulations of sinusoidal carriers, the FRF model with typical octave-wide first-stage filters is inadequate for explaining human sensitivity to high-frequency texture modulation.

Band-pass filtering and rectification of a texture-defined image is a low-pass operation on the recovered modulator. To see this, consider a simple contrast-modulated texture like that shown in Fig. 2A. The carrier and modulator, with frequencies f_c and f_m respectively, are both sine waves, localized in spatial frequency and orientation. In the frequency domain the modulator manifests as a pair of distortion products displaced a distance f_m away from the carrier in a direction determined by the orientation of the modulator, resulting in sidebands that differ in frequency and potentially in orientation from the carrier. A typical psychophysical channel is Gaussian with sensitivity falling off from its preferred spatial frequency and orientation. Because high-frequency modulators are, in the Fourier domain, displaced a significant distance from the carrier, they are attenuated greatly by a first-stage filter matched to the carrier. In spatial terms, the Gabor filters that underlie a psychophysical channel are large relative to the contrast-defined stripes, and blur out variations of texture.

Because V1 channels have fixed bandwidth in octaves, this blurring depends on the ratio of modulator to carrier frequency, and may provide a parsimonious explanation for scale invariance in second-order vision. However, unless sensitivity to high-frequency second-order modulation is somehow restored by downstream highpass filtering, sensitivity to second-order images should fall off dramatically as modulator frequency increases relative to carrier frequency (Fig. 3). Measurements of the second-order contrast sensitivity function (CSF) using a variety of second-order stimuli are somewhat inconsistent, but are generally either nearly flat (Landy & Oruç, 2002; Sutter, Sperling, & Chubb, 1995) or modestly low pass (Jamar & Koenderink, 1985; Kingdom, Keeble, & Moulden, 1995; Schofield & Georgeson, 2003), although more dramatically low-pass sensitivity profiles have been found (Schofield & Georgeson, 1999). Measured sensitivity to high-frequency modulation is usually somewhat better than would be predicted by a FRF model that uses a single carrier-matched first-stage channel, and in some cases the difference is dramatic. In the study using orientation-modulated stimuli most similar to those considered here, Landy and Oruç (2002) found the second-order CSF to be almost flat over a 5 octave range (Fig. 4), which is totally inconsistent with the use of a single first-order channel matched to the carrier.

We propose that the higher than expected sensitivity of the human visual system to high-frequency texture modulation can be explained by a first stage of filtering that pools over many nearby channels, so that sensitivity to orientations and frequencies slightly different from the carrier is relatively constant (Fig. 2C) and effective bandwidth is very high. Fig. 5 shows the effect of the second-order blurring we describe on a sample image, as well as an example of how pooling over first-order channels can

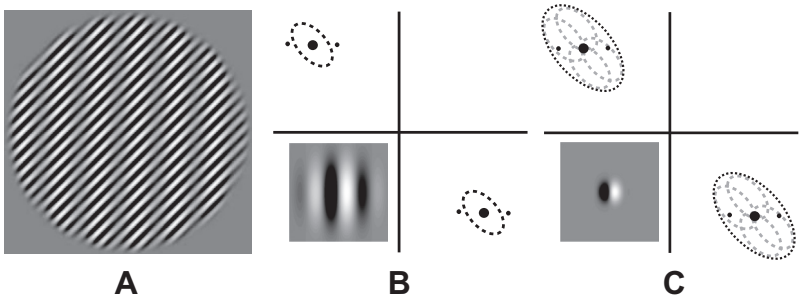

Fig. 2. (A) Example contrast-modulated stimulus. (B) A schematic of its Fourier transform. The distance of each sideband from the carrier is equal to the modulation frequency and the orientation of the displacement of these sidebands from the carrier is equal to the modulator orientation. With increasing modulator frequency, the sidebands will fall outside the bandwidth of the hypothetical first-stage filter (shown in (B) by the dotted line). (C) If the first-stage filter pools over many channels, high-frequency modulators will be less attenuated. Shown inset are the spatial filters corresponding to a single channel (B) and the resulting broad-bandwidth pooled channel (C). Note that as tuning bandwidth increases the size of the spatial receptive field becomes smaller, leading to reduced spatial blurring under the FRF model.

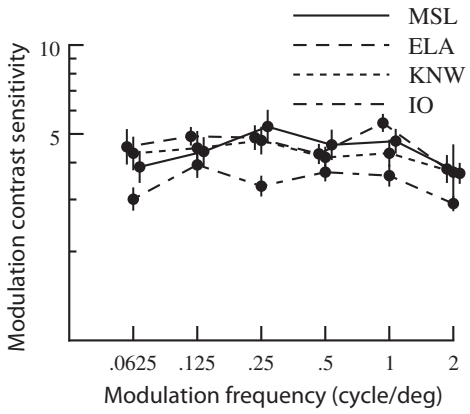

Fig. 4. Figure from Landy and Oruç (2002) showing nearly flat second-order contrast sensitivity functions for four subjects. Carrier frequency is 4 cycle/deg.

mitigate the loss of high second-order frequencies. We simulated the modulation CSF (Fig. 3) for the single carrier-matched channel model of first-stage filtering, as well as two variants of the pooling model. Details of the simulation are described below (see Section 4). Both implementations of pooling models predict much flatter contrast sensitivity functions than the single-channel FRF model, and more closely match human performance. In this paper, in two experiments we provide psychophysical evidence that second-order mechanisms are not limited to a single, fixed, first-order input, and that they include input from first-order channels tuned away from the carrier to detect high-frequency modulations.

2. Experiment 1

2.1. Introduction

A significant source of evidence for independent channels is spatial-frequency- and orientation-specific adaptation. Long term viewing of a grating, for example, selectively decreases sensitivity to gratings that are similar in spatial frequency and orientation. Adaptation corresponds to a long-term suppression of activity in a subpopulation of neurons that are responsive to the adapting stimuli. Psychophysical and fMRI adaptation experiments have provided evidence for orientation (Larsson, Landy, & Heeger, 2006) and frequency (Hallum, Landy, & Heeger, 2011) tuning of second-order mechanisms. When applied to first-order stimuli like gratings, threshold elevation due to spatial-frequency adaptation elevates thresholds for a range of frequencies centered on the adapter with a half-height bandwidth of around 1.5 octaves (Blakemore & Campbell, 1969; Movshon & Blakemore, 1973; Stromeyer et al., 1982), although under some conditions the spread of adaptation can extend to 2 octaves before falling off (Snowden & Hammett, 1996).

Langley, Fleet, and Hibbard (1996) conducted an experiment designed to demonstrate a first stage of filtering before rectification. Subjects adapted to a first-order grating and then were asked to detect second-order contrast modulation of a sinusoidal carrier texture. Threshold elevation was maximal for adapters that were matched in spatial frequency and orientation to the target carrier. Although the spread of this adaptation was large, suggesting pooled first-stage filters, interpretation of the result is problematic because carrier contrast was varied rather than modulation contrast. Second-order modulation detection is remarkably insensitive to modest variation of carrier contrast (Barbot,

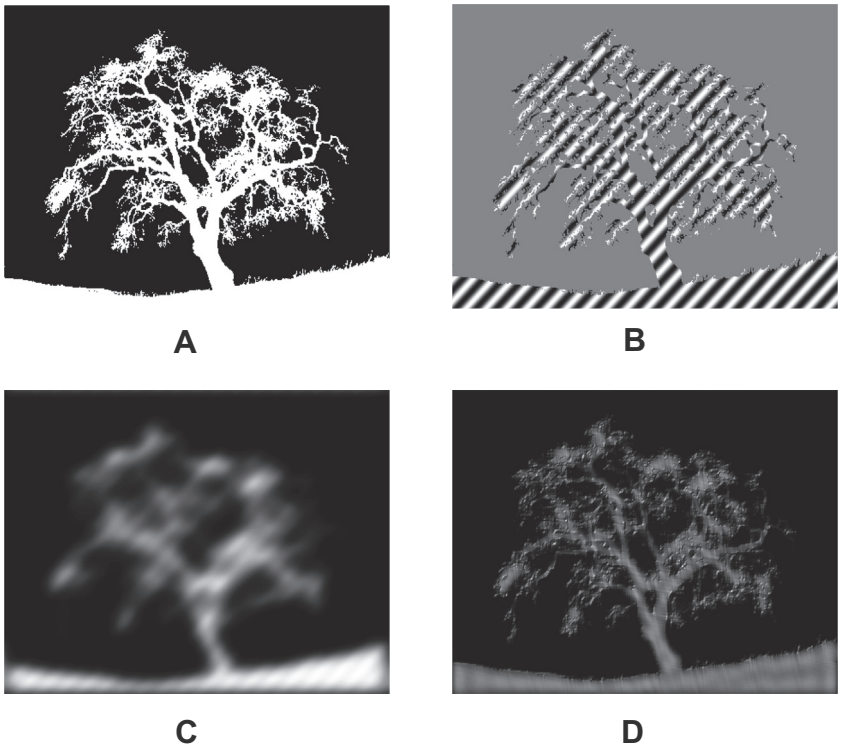

Fig. 5. Effect of first-stage filtering and rectification. (A) A "first-order" tree. (B) Corresponding second-order tree using a diagonal carrier texture. (C) Filtering and rectification of (B) by a single first-order channel tuned to the carrier with typical bandwidth for V1 results in an extremely blurred tree. (D) Use of a broadband first-order filter produces a much sharper demodulated image. See Fig. 2 for examples of narrowly and broadly tuned first-stage filters.

Landy, & Carrasco, 2011). Because adaptation is usually thought of as equivalent to a reduction in contrast, it is not clear how adapting to a first-order grating should affect second-order performance. Moreover, results of Langley's study are consistent with adaptation occurring in a first-order mechanism rather than necessarily in a second-order mechanism for which the first-order stage provides input.

In Expt. 1 we demonstrate that second-order mechanisms receive input from a wide-range of first-order spatial frequencies using second-order pattern adaptation. Several studies have established orientation-specific second-order adaptation (Kwan & Regan, 1998; Larsson, Landy, & Heeger, 2006). In the experiment, the second-order adapting stimulus has a fixed carrier frequency, while the adaptation effect is measured for test second-order gratings at several different carrier spatial frequencies. By measuring orientation-specific adaptation effects between adapter and test gratings that differ in carrier frequency, we can measure the range of spatial frequencies over which second-stage filters receive first-order input. Note that we could in principle have varied carrier orientation in order to demonstrate broad first-order tuning, but this would have prevented the use of orthogonal carriers rotated equally with respect to the modulator. Because second-order performance is nearly invariant to first-order contrast, it is unclear what the effects of first-order adaptation would be, and so we would like to rule out any potential first-order effect. We balance the design for the effects of first-order adaptation by measuring differential adaptation of second-order stimuli that have identical first-order content but which have either the same or orthogonal second-order orientation relative to the adapter.

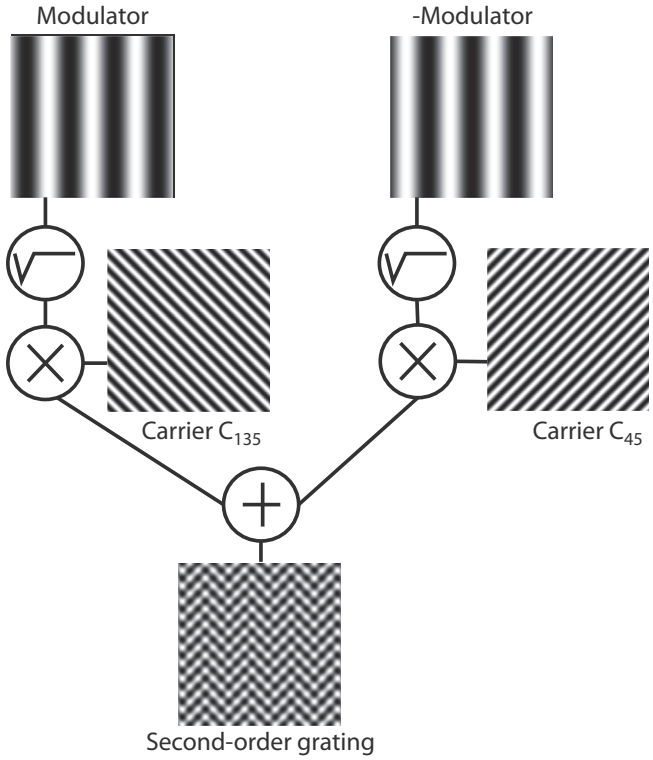

Fig. 6. Stimulus construction of orientation-modulated sine-wave gratings. Stimuli consist of sinusoidal carriers at 45° and 135° modulated in contrast with opposite phase and summed to produce an orientation-modulated image. The square root ensures that local root-mean-square contrast is constant across the image.

2.2. Methods

2.2.1. Stimuli

Stimuli are orientation-modulated sine-wave gratings with oblique sine-wave carriers. Fig. 6 shows a schematic stimulus-construction diagram. Oblique carriers C_{45} and C_{135} have spatial frequency f_c. Modulators M_0 and M_{90} were horizontal and vertical sine-wave gratings of spatial frequency f_m. The stimulus $C(x,y)$ is then defined as

$$\begin{aligned} M(x,y) &= \begin{cases} \sin(f_m x + \phi) & \text{if } M = M_0 \\ \sin(f_m y + \phi) & \text{if } M = M_{90} \end{cases} \\ m_1(x,y) &= C_{45}(x,y)\sqrt{\frac{1}{2}(1 + c_m M(x,y))} \\ m_2(x,y) &= C_{135}(x,y)\sqrt{\frac{1}{2}(1 - c_m M(x,y))} \\ C(x,y) &= 1 + m_1(x,y) + m_2(x,y), \end{aligned} \tag{1}$$

where c_m is second-order modulation contrast, which was varied across trials to determine second-order modulation-contrast threshold. The stimulus C was scaled to fully span the (0,255) pixel range. The square root ensures that local root-mean-square contrast is constant across the image, so that an early luminance nonlinearity, prior to linear filtering, would be unhelpful in detecting the second-order modulation. The use of pure sine waves for the modulator and carrier means that both are localized in the frequency domain, so that a single matched first-stage filter is unambiguously defined, and avoids contrast modulations associated with the use of filtered-noise carriers (Kovács & Fehér, 1997).

Stimuli were displayed on a Diamond Pro 900u CRT monitor with a viewing distance of 64.5 cm, so that the stimuli subtended 15° × 15°, and an average luminance of 17.5 cd/m^2. A linearized lookup table was used to adjust for monitor gamma. Stimuli were windowed by a circular raised cosine (cosine width: 1.25°) to reduce edge effects.

2.2.2. Procedure

Each block began with 100 s of adapter stimuli (as in Larsson, Landy, and Heeger (2006)). The adapter was a second-order grating with 70% modulation contrast. Every 500 ms a new grating was displayed with second-order phase chosen randomly and uniformly. The modulator and carrier frequencies and orientation of the adapter were fixed across each experimental session. Each subject was run in a session with a 0° adapter and in a session with a 90° adapter.

Each trial began with a 4 s top-up adapter to maintain the adaptation state, then two stimuli were shown for 500 ms each with a 250 ms blank interval between. One stimulus contained a second-order grating of either 0° or 90° orientation, while the other stimulus was an unmodulated plaid. The subjects' task was to indicate with a button press which interval contained the second-order grating. Although the adapter and target modulation frequency were always identical, their carrier spatial frequencies could differ, allowing us to test for cross-adaptation (Fig. 7). Within a session, a single modulation frequency and a single pair of test and adapter carrier frequencies were used. Modulation contrast was varied by two interleaved 1-up 2-down staircases, one for each modulator orientation. In separate sessions, four subjects were tested with a 6 cycle/deg adapter carrier, 1.5, 3 and 6 cycle/deg test carriers and the modulator frequency was one-third of the test carrier frequency. Two of these subjects were also tested with an 8 cycle/deg adapter carrier, 2, 4 and 8 cycle/deg test carriers and 0.5 cycle/deg modulator.

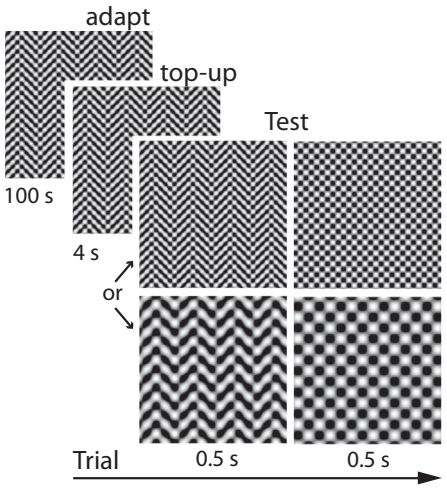

Fig. 7. Block and trial structure. Before each block, the adapter was displayed for 100 s, with a new adapter with random modulator phase presented every 0.5 s. Each trial consisted of a 4 s top-up adapter followed by two 0.5 s test stimulus intervals, each preceded by a 250 ms blank interval. One test interval, chosen randomly, contained an unmodulated plaid and one contained a modulated grating. Test modulation frequency was always the same as for the adapter, but test carrier frequency could be either the same as the adapter's (top row) or lower (bottom row), and test modulator orientation could be identical to the adapter or orthogonal. The subject's task was to indicate which interval contained modulation.

2.2.3. Analysis

Data pooled within each condition were fit with a Weibull psychometric function by maximum likelihood, and threshold was defined as the modulation contrast necessary to attain 75% correct. Our measure of adaptation was defined as follows:

$$\text{Adaptation index,}\quad I_{\text{adapt}} = \frac{T_0^{90} + T_{90}^{0}}{T_0^{0} + T_{90}^{90}}, \tag{2}$$

where T_0^{90} was the threshold of the 0° target viewed following a 90° adapter, and the other terms are defined analogously. An I_{adapt} of less than one corresponds to the expected effect of adaptation if target and adapter are processed by the same second-order mechanisms, while an index of 1 corresponds to no orientation-specific adaptation. Crucially, any adaptation measured this way can only result from mechanisms selective for second-order orientation, because the numerator and denominator of I_{adapt} differ only with respect to the orientation of the adapter's modulation orientation relative to that of the test. Any effects of adaptation to the first-order carriers should cancel out in the calculation of I_{adapt}. Confidence intervals were obtained by resampling the data from each condition with a parametric bootstrap (Maloney, 1990) and recomputing thresholds 400 times. Error bars on graphs represent 95% confidence intervals.

2.2.4. Subjects

Four subjects, AB, EKC, MSL, and ZMW, took part in this experiment. Two, ZMW and MSL, were authors. All subjects had corrected-to-normal visual acuity. The Institutional Review Board at New York University approved the experimental procedures and all participants gave informed consent.

2.3. Results

For the conditions using the adapter with the 8 cycle/deg carrier, subject ZMW had a significant adaptation effect with an 8 cycle/deg carrier test, but not with 2 or 4 cycle/deg tests, although for each the data were in the direction indicating an adaptation effect (Fig. 8). Subject MSL also ran in this condition, and displayed significant adaptation effects even with the 2 cycle/deg carrier target. This inconsistency may be due to the relative difficulty of seeing an 8 cycle/deg grating, reducing the effectiveness of the adapter. In the 6 cycle/deg adapter conditions, subjects AB, ZMW, and EKC showed significant adaptation effects in the 6, 3 and 1.5 cycle/deg carrier conditions, except for only a trend for AB in the 3 cycle/deg carrier condition ($p = 0.06$). Pooled over subjects, there is significant adaptation for every combination of adapter and test carrier frequency.

We have evidence for cross-carrier adaptation even when the carriers of the adapt and test stimuli differ dramatically in spatial frequency. Based on the design of our adaptation index, these results cannot reflect effects of adaptation that is not tuned for second-order orientation or adaptation specifically to the carrier. In conditions in which the two carriers differ only by an octave (8 cycle/deg adapter and 4 cycle/deg test carrier frequencies or 6 cycle/deg adapter and 3 cycle/deg test carrier frequencies) it is possible that first-stage filters tuned to intermediate frequencies between the adapter and target could participate in the detection of both. But, such an explanation is ruled out by the results of conditions in which adapter and test carrier frequencies differ by two octaves. This was especially true because the adapter had higher frequency than the target, and a channel centered on a low-frequency target is narrower in absolute bandwidth, and thus has very little sensitivity to the adapter's carrier. Thus, individual orientation-tuned second-order mechanisms must receive inputs from multiple first-order channels to explain these results.

3. Experiment 2

3.1. Introduction

Although Expt. 1 demonstrates invariance to carrier frequency for cross-adaptation, it does not necessarily follow that the extent of pooling implied by cross adaptation reflects mandatory broadband pooling of first-order filters as input to second-order mechanisms. A flexible second-order mechanism that can select input from any first-order channel, but which does not pool over multiple channels simultaneously, would be consistent with our adaptation results by allowing the same second-order mechanism to select different inputs in the adapt and test phases of the experiment. Such a second-order mechanism would adapt during the adaptation phase, while using a first-order filter tuned to the adapting grating's carrier, and would then show reduced sensitivity to the test stimulus, while using a first-order filter tuned to the test grating's carrier. The results of Expt. 1 are also consistent with a second-order mechanism that uses first-stage filters selective for orientation but not for spatial frequency. We are interested in the role that pooling may have for processing high-frequency modulators, which we address in Expt. 2 by measuring the second-order CSF in a condition designed to impair pooling.

We propose that the first-order input to second-order mechanisms is a broadly tuned filter composed of the sum of several ordinary psychophysical channels. At moderate contrast these channels are approximately linear, so that second-order channel response is proportional to first-order contrast. Because the filter includes channels tuned near the modulation sidebands, sensitivity to high- and low-frequency modulation is identical. Suppose that first-order contrast is reduced to near detection threshold, so that the carrier is barely visible. A widely observed effect in contrast discrimination performance is the dipper function, or a decrease in just-noticeable contrast difference near threshold (Solomon, 2009). Several explanations have been proposed for this dip, including the existence of an absolute sensory threshold (Green, 1974), an accelerating nonlinear transducer function (Bar-

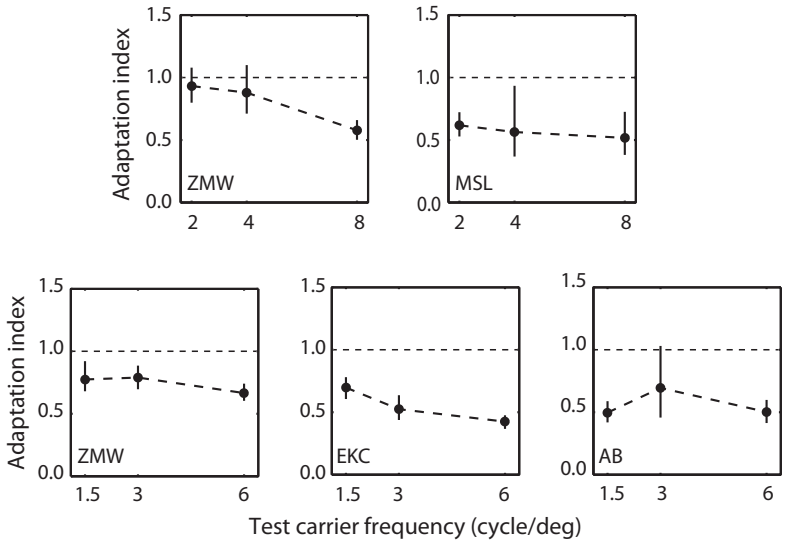

Fig. 8. Adaptation indices for all subjects in all conditions. Top row: 8 cycle/deg adapter carrier frequency. Bottom row: 6 cycle/deg adapter carrier frequency. Adaptation indices below one indicate cross-adaptation. Error bars represent 95% confidence intervals computed by bootstrap.

low et al., 1987; Legge & Foley, 1980), stimulus uncertainty leading to the consideration of irrelevant channels (Pelli, 1985), or hinge noise (Sanborn & Dayan, 2011). We assume an accelerating nonlinearity near threshold, which is supported by psychophysics and neurophysiological measurements of the contrast response function for individual neurons (Barlow et al., 1987). This nonlinearity would act to suppress responses of very weakly stimulated channels. Our proposed first-stage filter is composed of several first-order channels, some of which are tuned near the modulation sidebands. For high-frequency modulations, these sideband-tuned components are both essential in detecting the modulator, and are very weakly sensitive to the carrier. Because these sidebands contain far less power than the carrier, at very low contrasts their responses will fall into the nearly flat, "sub-threshold" range of the accelerating nonlinearity, effectively removing these channels from the pooled filter (Fig. 9). Note that our nonlinearity only needs to affect signals at undetectable or nearly undetectable contrasts to produce the observed effects: at 20% modulation contrast and 0.75% carrier contrast, for example, the sidebands are extremely low contrast (0.075%) gratings.

In Expt. 2, we measure a sample of the modulation contrast sensitivity function at several different first-order contrasts. Carriers are always 4 cycle/deg, while the modulator is either 0.5 cycle/deg or 1.5 cycle/deg. If responses are based on pooling of multiple first-order channels, each of which is affected by a low-contrast transduction nonlinearity as discussed above, then we predict that reducing contrast will reduce sensitivity to high- more than to low-spatial-frequency modulators.

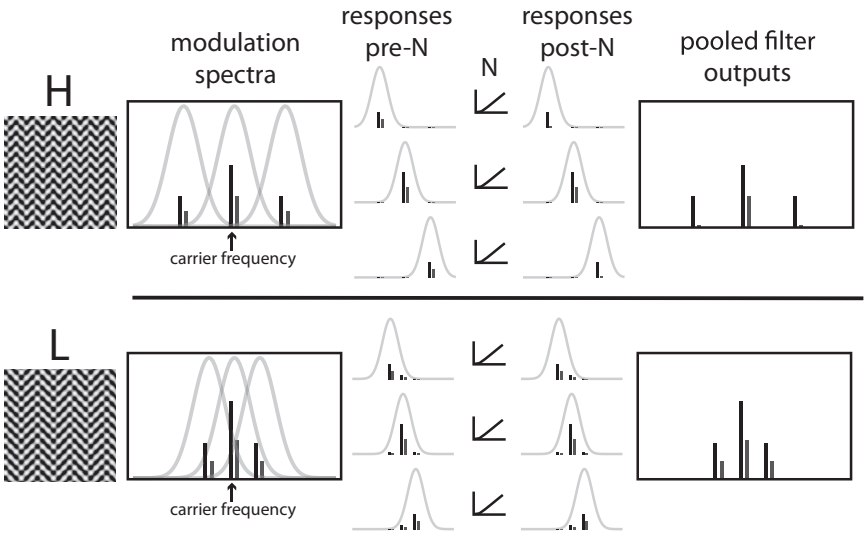

Fig. 9. Example spectra for contrast-modulated sine waves at different modulation frequencies along with channels making up a proposed pooled first-stage filter. In the Fourier domain, contrast modulation is made up of energy at the carrier frequency along with two weaker sidebands, offset by an amount equal to the modulation frequency. In the case of contrast modulated gratings, 100% modulation contrast sidebands each have half the amplitude of the carrier. High and low frequency modulation spectra are shown for high (black bars) and low first-order contrast (gray bars). The proposed nonlinearity at the level of individual first-order channels is insensitive to very low contrasts and responds nearly linearly above this point. 'Responses pre-N' shows linear responses within each first-order channel, while 'Responses post-N' shows responses after application of the nonlinearity. When first-order contrast is high, this nonlinearity has no effect. For high-frequency modulation of low-contrast first-order gratings, this nonlinearity eliminates responses of channels tuned to the modulation sidebands. For low-frequency modulation of low-contrast first-order gratings, first-order channels tuned to the sidebands are sensitive enough to energy at the carrier frequency that their overall responses are not eliminated. As a result, modulation sidebands are lost at low contrast only for high-frequency modulations, leading to a predicted loss of sensitivity to high-frequency modulators at low first-order contrasts.

3.2. Methods

3.2.1. Stimuli

The stimuli were orientation-modulated sine wave gratings as in Expt. 1, with reduced first-order contrast. Low contrast was achieved by altering the monitor gamma lookup table, and by alternating stimulus frames with uniform mean gray at 100 Hz. This produced stimuli that were presented at approximately 0.75%, 1.5%, and 3% contrast, without dramatic quantization artifacts. Modulators were either low-frequency (0.5 cycle/deg, Fig. 10A) or high-frequency (1.5 cycle/deg, Fig. 10B) gratings. Carriers were always 4 cycle/deg, near the peak of the first-order CSF.

3.2.2. Procedure

The task was to discriminate second-order grating orientation (vertical or horizontal). Each session consisted of three blocks of either the high- or low-frequency modulator at one of three different first-order contrast levels. Every five trials there was a high second-order contrast (70%) reminder trial. Each block consisted of 100 trials of two interleaved 1-up 2-down staircases that controlled modulation contrast. Because the first-order contrast was extremely low, one subject could not perform the task (never reached threshold performance) in the lowest of the three contrast conditions and was excluded.

3.2.3. Analysis

As in Experiment 1, data pooled within each condition were fit with a Weibull psychometric function. Threshold was defined as the modulation contrast necessary to attain 75% correct, and 95% confidence intervals were generated via bootstrapping. To clearly show the effect of first-order contrast on relative performance for high- and low-frequency second-order gratings, we computed the ratio of modulation contrast threshold of high- and low-frequency modulators. A ratio above one represents worse performance on high-frequency modulators. A negative slope of this ratio plotted as a function of first-order contrast suggests that, as one decreases first-order contrast, high-frequency sensitivity is degraded relative to low-frequency sensitivity.

3.3. Subjects

Four subjects took part in this experiment. One, ZMW, was an author and the other three were naive as to the purposes of the experiment. All subjects had normal or corrected-to-normal vision. The Institutional Review Board at New York University approved the experimental procedures and all participants gave informed consent.

3.4. Results

As expected under the pooling model, reducing carrier contrast selectively degraded orientation-discrimination performance for high-frequency modulators. Fig. 11 shows threshold ratio (the ratio of high- to low-frequency modulation contrast threshold) as a function of contrast. For every subject there is a clear effect of degraded high-frequency performance at low first-order contrasts, consistent with a lowpass effect on texture modulation sensitivity due to a reduced ability to pool over first-order channels at low contrast. Two subjects were more sensitive to the high-frequency grating in the highest first-order contrast condition (3.0%), while two were equally sensitive to high and low frequencies in this condition. We currently do not have an explanation for this difference in initial sensitivity. All subjects were, as expected, more sensitive to the low-frequency grating than to the high-frequency grating in the lowest-contrast condition (0.75%).

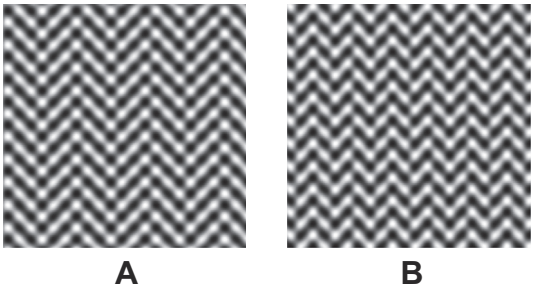

Fig. 10. Example stimuli that share the same carrier frequency but differ in modulation frequency.

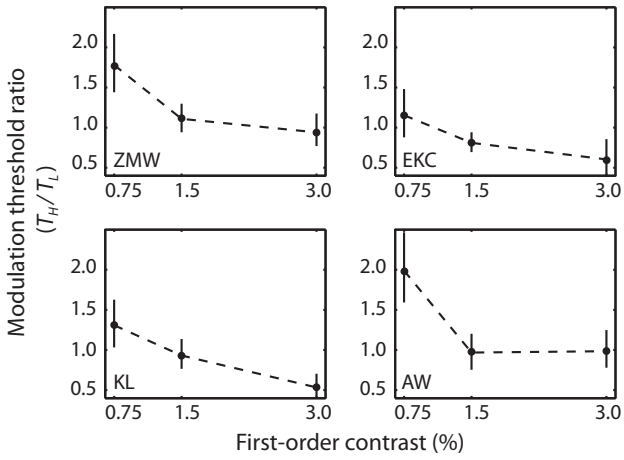

Fig. 11. Ratio of orientation-discrimination thresholds for high- (1.5 cycle/deg) and low-frequency (0.5 cycle/deg) second-order gratings at three different first-order contrast levels. As first-order contrast is reduced, relative sensitivity to high-frequency second-order gratings is also reduced.

Based on previous studies that varied first-order contrast for second-order gratings (Barbot, Landy, & Carrasco, 2011; Schofield & Georgeson, 1999), we expected that decreasing carrier contrast should have relatively little effect on sensitivity to low-frequency second-order modulation. This was confirmed for three of our four subjects, with only one subject showing a significant difference in sensitivity between the 0.75%- and 3%-contrast conditions. In the FRF model, second-order channel responses are approximately proportional to first-order contrast, but there are no explicit assumptions about the source of limiting noise. The relative contrast invariance of second-order processing may reflect Weber's law like behavior, indicating a dominant role of early multiplicative noise. Alternatively, it may be evidence for normalization of first-order inputs before they are processed by second-stage filters.

4. Modelling

4.1. Simulated orientation-modulation CSF

To model the effect of first-stage filtering, we simulate an FRF observer. The observer operated by filtering and rectifying the image with filters sensitive to each carrier to produce a texture-energy image, and then filtering again with a one-octave bandwidth second-stage filter matched to the spatial frequency and orientation of the modulation. We compute percentage correct based on this filter's response and fixed-variance additive Gaussian late noise. Because the second-stage filter was always exactly matched to the modulator spatial frequency, its bandwidth was not critical to our results. To examine the effects of different first-stage filters on sensitivity to orientation modulation, we

simulated three different FRF models. For model i, $E_i(x,y)$ denotes the texture-energy image, or demodulated image, immediately preceding second-stage filtering.

1. A single-channel model. In this model filters consist of a quadrature pair of Gabor filters tuned to the orientation and spatial-frequency of each carrier. Each filter had half-height bandwidths of one-octave and 30°.

$$E_1(x,y) = \left[\left(I * f_{45}^0\right)^2 + \left(I * f_{45}^{\pi/2}\right)^2\right] - \left[\left(I * f_{135}^0\right)^2 + \left(I * f_{135}^{\pi/2}\right)^2\right], \quad (3)$$

where I is the input image, f_{45}^0 and $f_{45}^{\pi/2}$ are the filters tuned to the 45° carrier in cos and sin phase respectively (and likewise for the 135° carrier), $*$ represents convolution, and the sum of squared outputs from each quadrature pair yields a measurement of texture energy.

2. An early-pooling model. First-stage filters are a quadrature pair of filters that are locally flat in the Fourier domain. The filters have finite bandwidth, so that the filter tuned to one carrier excludes the orthogonal carrier. This model corresponds to pooling across first-order channels near the carrier before rectification. Because there was almost no stimulus energy past the sidebands, the exact filter design was not important. We simply used Gabor filters thresholded at a low value. This is not intended to represent a realistic pooled filter, which would not be sharp-edged in the Fourier domain, but for the purposes of model simulation the choice does not matter so long as the resulting filters encompass all of the energy within each carrier band.

$$E_2(x,y) = \left[\left(I * \sum_{i\in F_{45}} f_i^0\right)^2 + \left(I * \sum_{i\in F_{45}} f_i^{\pi/2}\right)^2\right] - \left[\left(I * \sum_{i\in F_{135}} f_i^0\right)^2 + \left(I * \sum_{i\in F_{135}} f_i^{\pi/2}\right)^2\right], \quad (4)$$

where F_{45} and F_{135} are the sets of filters tuned near the 45° and 135° carriers.

3. Post-rectification pooling. First-stage filters are constructed as in model 1, but the image is processed by 9 filters with preferred orientation and spatial-frequency evenly tiled near one of the carriers. After rectification, the 9 filter outputs are summed:

$$E_3(x,y) = \sum_{i\in F_{45}}\left[\left(I * f_i^0\right)^2 + \left(I * f_i^{\pi/2}\right)^2\right] - \sum_{i\in F_{135}}\left[\left(I * f_i^0\right)^2 + \left(I * f_i^{\pi/2}\right)^2\right]. \quad (5)$$

Filters were laid out in a grid so that the central filter matched the carrier, with the grid spaced such that two locations coincided with the modulation sidebands.

The use of quadrature-pair filters and squaring for rectification means that, for the single-channel case, the demodulated image is analogous to the response of carrier-tuned complex cells across space. We subtracted responses of the two orientations to produce an orientation-opponent signal (Bergen & Landy, 1991). Because both orientation channels contain identical information, a model that uses only filters tuned to one of the carriers produces nearly identical predictions. After rectification we simulate the effects of second-stage filtering on the resulting texture-energy images by computing the energy in a second-stage channel tuned to the modulator. The output of the second-stage channels is corrupted by Gaussian noise with SD chosen to produce human-like thresholds. We compute percentage correct at each modulation contrast, fit a Weibull psychometric function, and report sensitivity as the reciprocal of the modulation contrast corresponding to 75% correct performance.

Fig. 3 shows a simulated second-order modulation CSF for each model using a 4 cycle/deg carrier. For each model, we chose a level of late noise that equated performance in the lowest-frequency condition. There is a dramatic drop in sensitivity for the single-channel model from 0.25 to 1.75 cycle/deg. Across the same range, the early-pooling model's performance is flat, and the post-rectification-pooling model's performance is intermediate. The flatness of the modulation CSF for the early- and late-pooling models depends on the choice of channels to pool over and the weights assigned to those channels. The early-pooling model shown here should therefore be interpreted as the limiting case for pooling as a means of achieving a flat CSF; a different choice of weights and channels can easily produce low-pass behavior.

The relationship between channel weights and the resulting CSF in the late-pooling model is less clear, due to the intervening nonlinearity (see Fig. 9 for an example of how a simple nonlinearity can distort apparent channel shape). We took no particular care to choose a set of channels that maximized the flatness of the simulated CSF. The intent of the late-pooling model is to show that pooling after rectification can result in a considerable gain in high-frequency sensitivity, resulting in a modestly low-pass modulation CSF that agrees with several existing measurements. The late-pooling model is appealing because it avoids some of the issues with phase-alignment and negative firing rates that would complicate implementation of early pooling with realistic neurons. It can be thought of as a straightforward energy summation model, or as the result of probability summation between independent mechanisms (i.e., independent second-order mechanisms with different first-order inputs).

4.2. Simulated contrast-modulated noise CSF

Existing reports of the modulation CSF range from nearly flat (Landy & Oruç, 2002; Sutter, Sperling, & Chubb, 1995), to modestly lowpass (Jamar & Koenderink, 1985; Kingdom, Keeble, & Moulden, 1995; Schofield & Georgeson, 2003), to dramatically lowpass (Schofield & Georgeson, 1999). Although we cannot definitively resolve the inconsistency, our modelling suggests that differences in the shape of the modulation CSF may result from the use of different carrier textures. Schofield and Georgeson (1999) measured the

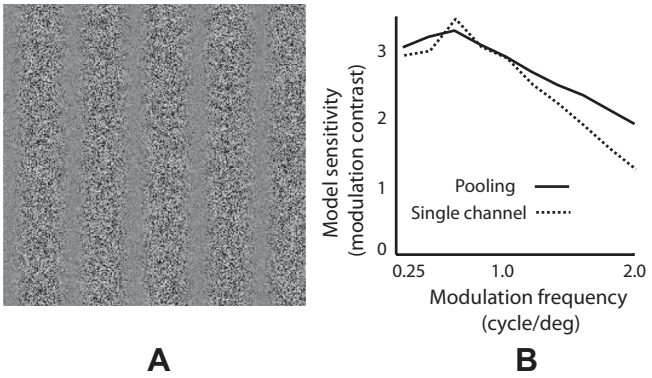

Fig. 12. (A) Contrast-modulated white-noise grating. (B) FRF model CSFs in response to contrast modulation of white noise (solid: single-channel model; dashed: early-pooling model). For contrast-modulated white noise, pooling does not flatten the CSF to nearly the same degree as for orientation-modulated stimuli with sinusoidal carriers.

modulation CSF of contrast-modulated white noise (similar to Fig. 12A) and found it to be very low pass. Applying the FRF model to second-order patterns defined by white noise carriers is difficult, because there is no non-arbitrary choice of first-stage filter. If we assume, however, that observers use a single channel with arbitrary orientation tuning and frequency tuning near the peak of the first-order contrast sensitivity function (4 cycle/deg), we can simulate the FRF model as we did for orientation-modulated images to obtain a predicted contrast modulation CSF. Fig. 12B shows the result of this simulation: a low-pass modulation CSF as expected based on the available human data. If we simulate an early-pooling FRF model with broad first-stage filters, we obtain nearly the same result (Fig. 12B). In contrast, when the carriers were diagonal gratings, the early-pooling FRF observer had a flat modulation CSF (Fig. 3). Pooling over multiple first-stage filters fails as a strategy for avoiding loss of high-frequency sensitivity when carriers are broadband noise. This may explain why the modulation CSF is nearly flat for orientation-modulated gratings (Landy & Oruç, 2002) but is low-pass to varying degree for other stimulus configurations.

5. Discussion

We have shown that, under the standard FRF model, second-order images are essentially blurred by the envelope of the first-stage filter. Because mechanisms responsible for texture demodulation are selective for the spatial-frequency and orientation of the carrier (Dakin & Mareschal, 2000; Langley, Fleet, & Hibbard, 1996; Prins & Kingdom, 2002) in much the same way as first-order channels are selective for spatial-frequency and orientation, it is tempting to imagine that the first-stage of filtering in FRF is carried out by typical V1 simple cells with frequency and orientation tuning matched to the carrier texture. Because of the interaction we have discussed between first-order bandwidth and second-order sensitivity, using a single first-order channel as first-stage filter would produce a modulation contrast-sensitivity function that is dramatically low-pass. Measurements of the human modulation contrast-sensitivity function range from lowpass to nearly flat, but sensitivity to high-frequency modulators is generally much higher than would be predicted under the FRF model with a single first-order channel per carrier serving as first-stage filter. For orientation-modulated sine wave gratings similar to those considered here, the modulation CSF is nearly flat over a five-octave range (Landy & Oruç, 2002).

We propose that the higher-than-expected visibility of high-frequency second-order gratings is due to a first stage of filtering that pools over a set of channels tuned near the carrier. By pooling over these channels, the visual system can retain just enough orientation tuning to discriminate orthogonal carriers without being so narrowly tuned as to filter out the sidebands that signal modulation. Our modelling results suggest that a wideband pooled first-stage filter can recover high-frequency sensitivity in simulations of the FRF model on orientation-modulated gratings, but that this strategy may not be helpful with contrast-modulated noise textures, possibly explaining the variability in measurements of the human modulation CSF.

In Experiment 1 we considered an implication of wideband first-stage filters on cross-adaptation between stimuli that differ in carrier spatial frequency. If second-stage filters receive rectified input from V1 simple cells tuned only to the carrier's orientation and frequency, stimulus pairs with carriers that fall outside of each other's respective channels should not activate overlapping populations of second-stage filters. If instead the second-stage filters receive input from a relatively broad range of first-order orientations and frequencies, we would expect the same second-stage filters to be sensitive to stimuli that differ in first-order properties of the carrier. We tested for such carrier invariance using adaptation, and demonstrated cross adaptation for carrier frequencies that differed by a factor of four.

This result demonstrates that individual second-order mechanisms receive input from first-stage filters with very different tuning properties, but does not on its own demonstrate pooling. Each second-order mechanism could instead select on each trial relevant first-order inputs. Flexible input selection may in fact be necessary to explain sensitivity to other types of second-order images. The lowpass effect of first-stage filtering with narrowband filters represents a tradeoff between spatial resolution in the demodulated second-order image and orientation/frequency resolution in isolating a carrier. For orientation-modulated images using orthogonal carriers and relatively high modulation frequencies, the optimal choice is clearly to sacrifice first-order tuning in exchange for enhanced sensitivity to high-frequency modulation. However, when carriers have similar tuning properties, or when properties like frequency or orientation are modulated only slightly, broadly tuned first-stage filters would render second-order structure invisible. Given the visibility of frequency-modulated stimuli (Prins & Kingdom, 2002) and the narrow carrier-frequency selectivity exhibited in different second-order tasks (Kingdom & Keeble, 2000), it seems unlikely that the degree of carrier-frequency invariance observed here is a fixed property of all second-order mechanisms. Either the mechanisms we observed are distinct from those that serve to detect modulation between similar carriers, which requires narrow tuning, or there is a single set of mechanisms with flexible first-order tuning. Second-order filters may be able to select an optimal set of first-order inputs, a notion supported by evidence for summation between orthogonal carriers (Motoyoshi & Nishida, 2004) and by results showing the use of off-frequency tuned first-stage filters for detecting frequency modulations (Prins & Kingdom, 2002).

The results of Expt. 1 rule out two alternative hypotheses about the mechanisms responsible for second-order vision. Tanaka and Ohzawa (2009) found neurons in cat V1 that displayed selectivity to the properties of drifting second-order gratings, as well as first-order orientation and frequency tuning consistent with simple or complex cells. They showed that the second-order sensitivity of these neurons was due to asymmetric surround suppression. Several authors have suggested that second-order stimuli might be detected by purely linear mechanisms tuned to the sidebands (Dakin & Mareschal, 2000; Schofield & Georgeson, 2003), although a phase-randomization control ruled out this explanation for stimuli similar to those used here (Landy & Oruç, 2002). Explanations based on asymmetrical suppression and sideband-tuned filters both propose that first-order mechanisms tuned near the carrier are responsible for second-order sensitivity. Because we have demonstrated adaptation between stimuli whose carriers were very different, which produce very different sidebands and would activate a distinct set of first-order filters, it is unlikely that either of these carrier-centered mechanisms contributed much to second-order sensitivity.

In Expt. 2, we were interested in directly addressing the pooling hypothesis by creating stimulus conditions that make pooling over channels tuned to the modulation sidebands difficult. Based on evidence for the existence of a nonlinearity near threshold that suppresses weak responses for both psychophysical channels and neurons in V1 (Barlow et al., 1987), we proposed that as first-order contrast approaches carrier detection threshold, channels that overlap only slightly with the carrier, and which are stimulated only by the much lower contrast sidebands, will have their responses attenuated. Because these off-tuned channels carry most of the second-order signal for high-frequency-modulated stimuli, lowering first-order contrast should result in lowpass second-order modulation sensitivity. Indeed we found second-order contrast

sensitivity at 0.75% carrier contrast reduced significantly from sensitivity at 3% contrast for high-frequency second-order gratings.

The design and interpretation of Expt. 2 was based on the contrast response of visual channels and of simple cells in V1 at very low contrasts. An important concern is the extent to which channel tuning properties may change at low contrasts. At reduced contrast some neurons exhibit increased length summation (Fitzpatrick, 2000; Kapadia, Westheimer, & Gilbert, 1999; Sceniak et al., 1999). It is plausible that enlarged spatial summation may produce increased spatial blurring of the modulation signal, leading to a loss of high-frequency sensitivity similar to what we obtained in Expt. 2. Although we cannot rule out this explanation, we think it is unlikely to be responsible for our results. Significant enlargement of length summation has been observed at contrasts as high as 30% (Kapadia, Westheimer, & Gilbert, 1999). We assume that if length-summation effects were the cause of our results, then observers would already have been much less sensitive to high-frequency modulation with 3% contrast carriers, which was not true for any of our observers. Moreover, enlarged length summation is not equivalent to an enlargement of the cell's linear receptive field—stimuli in the summation region do not induce firing on their own—so it is unclear what effect enlarged length summation would have on spatial blurring of contrast-modulated signals.

In previous work we have shown that the standard FRF model cannot account for second-order critical-band masking data (Westrick, Henry, & Landy, 2013) and suggested the incorporation into the FRF of an additional nonlinearity that thresholds texture-energy responses. It may strike the reader as odd that this nonlinearity, which essentially labels each location according to the dominant carrier, is absent from the models presented here. We opted to simulate a more standard formulation of the FRF model because, at low modulation contrast and in the absence of a masker, the additional nonlinearity has a very minor effect on simulated behavior, as long as there is a small amount of early noise present. Crucially, the same low-pass effect of filtering with standard-bandwidth first-stage filters is observed in the more complicated FRF model with thresholding, as is the recovery of high-frequency content with broadband first-stage filters.

Our proposal of flexible first-order inputs to second-order mechanisms leaves unspecified how carrier-selection mechanisms determine which first-order channels should be pooled. Most studies of second-order vision avoid the issue by using fixed carriers, but the issue of first-order channel selection is important for models of texture perception. In general, only a subset of first-order channels are modulated by a second-order stimulus. Determining the relevant first-order inputs therefore requires information about modulator structure, which itself requires a selection of first-stage filters. A flexible system may therefore benefit from iterative processing, in which crudely demodulated image structure informs selection of carriers through feedback. An examination of human performance in texture segmentation under conditions of uncertainty about the carrier may be necessary to determine how input selection operates in general processing of texture-defined images.

Acknowledgment

We thank Christopher Henry and Ipek Oruç for comments on the manuscript. This work was supported, in part, by NIH grant EY08266.

References

Barbot, A., Landy, M. S., & Carrasco, M. (2011). Exogenous attention enhances 2nd-order contrast sensitivity. *Vision Research, 51*, 1086–1098.

Barlow, H. B., Kaushal, T. P., Hawken, M., & Parker, A. J. (1987). Human contrast discrimination and the threshold of cortical neurons. *Journal of the Optical Society of America A, 4*, 2366–2371.

Bergen, J. R., & Landy, M. S. (1991). Computational modeling of visual texture segregation. In M. S. Landy & A. J. Movshon (Eds.), *Computational models of visual processing* (pp. 253–271). Cambridge, Mass.: MIT Press.

Blakemore, C., & Campbell, F. W. (1969). On the existence of neurones in the human visual system selectively sensitive to the orientation and size of retinal images. *Journal of Physiology, 203*, 237–260.

Dakin, S. C., & Mareschal, I. (2000). Sensitivity to contrast modulation depends on carrier spatial frequency and orientation. *Vision Research, 40*, 311–329.

Fitzpatrick, D. (2000). Seeing beyond the receptive field in primary visual cortex. *Current Opinion in Neurobiology, 10*, 438–443.

Graham, N. (1994). Non-linearities in texture segregation. *Proceedings of the CIBA foundation symposium* (Vol. 184, pp. 309–323). New York: Wiley.

Graham, N., Sutter, A., & Venkatesan, C. (1993). Spatial-frequency- and orientation-selectivity of simple and complex channels in region segregation. *Vision Research, 33*, 1893–1911.

Green, D. M. (1974). *Signal detection theory and psychophysics*. Huntington, NY: R.E. Krieger Pub. Co.

Hallum, L. E., Landy, M. S., & Heeger, D. J. (2011). Human primary visual cortex (v1) is selective for second-order spatial frequency. *Journal of Neurophysiology, 105*, 2121–2131.

Jamar, J. H. T., & Koenderink, J. J. (1985). Contrast detection and detection of contrast modulation for noise gratings. *Vision Research, 25*, 511–521.

Kapadia, M. I., Westheimer, G., & Gilbert, C. D. (1999). Dynamics of spatial summation in primary visual cortex of alert monkeys. *Proceedings of the National Academy of Sciences of the USA, 96*, 12073–12078.

Kingdom, F. A. A., Keeble, D., & Moulden, B. (1995). Sensitivity to orientation modulation in micropattern-based textures. *Vision Research, 35*, 79–91.

Kingdom, F. A. A., & Keeble, D. R. T. (1999). On the mechanism for scale invariance in orientation-defined textures. *Vision Research, 39*, 1477–1489.

Kingdom, F. A. A., & Keeble, D. R. T. (2000). Luminance spatial frequency differences facilitate the segmentation of superimposed textures. *Vision Research, 40*, 1077–1087.

Kovács, I., & Fehér, A. (1997). Non-fourier information in bandpass noise patterns. *Vision Research, 37*, 1167–1175.

Kwan, L., & Regan, D. (1998). Orientation-tuned spatial filters for texture-defined form. *Vision Research, 38*, 3849–3855.

Landy, M. S., & Oruç, İ. (2002). Properties of second-order spatial frequency channels. *Vision Research, 42*, 2311–2329.

Langley, K., Fleet, D. J., & Hibbard, P. B. (1996). Linear filtering precedes nonlinear processing in early vision. *Current Biology, 6*, 891–896.

Larsson, J., Landy, M. S., & Heeger, D. J. (2006). Orientation-selective adaptation to first- and second-order patterns in human visual cortex. *Journal of Neurophysiology, 95*, 862–881.

Legge, G. E., & Foley, J. M. (1980). Contrast masking in human vision. *Journal of the Optical Society of America, 70*, 1458–1471.

Maloney, L. T. (1990). Confidence intervals for the parameters of psychometric functions. *Perception & Psychophysics, 47*, 127–134.

Motoyoshi, I., & Nishida, S. (2004). Cross-orientation summation in texture segregation. *Vision Research, 44*, 2567–2576.

Movshon, J. A., & Blakemore, C. (1973). Orientation specificity and spatial selectivity in human vision. *Perception, 2*, 53–60.

Pelli, D. G. (1985). Uncertainty explains many aspects of visual contrast detection and discrimination. *Journal of the Optical Society of America A, 2*, 1508–1532.

Prins, N., & Kingdom, F. A. A. (2002). Orientation and frequency-modulated textures at low depths of modulation are processed by off-orientation and off-frequency texture mechanisms. *Vision Research, 42*, 705–713.

Prins, N., & Kingdom, F. A. A. (2006). Direct evidence for the existence of energy-based texture mechanisms. *Perception, 35*, 1035–1046. article 9.

Sanborn, A. N., & Dayan, P. (2011). Optimal decisions for contrast discrimination. *Journal of Vision, 11*(14), 1–13. article 9.

Sceniak, M. P., Ringach, D. L., Hawken, M. J., & Shapley, R. (1999). Contrast's effect on spatial summation by macaque v1 neurons. *Nature Neuroscience, 2*, 733–739.

Schofield, A. J., & Georgeson, M. A. (1999). Sensitivity to modulations of luminance and contrast in visual white noise: Separate mechanisms with similar behavior. *Vision Research, 39*, 2697–2716.

Schofield, A. J., & Georgeson, M. A. (2003). Sensitivity to contrast modulation: The spatial frequency dependence of second-order vision. *Vision Research, 43*, 243–259.

Scott-Samuel, N. E., & Georgeson, M. A. (1999). Does early non-linearity account for second-order motion? *Vision Research, 39*, 2853–2865.

Snowden, R. J., & Hammett, S. T. (1996). Spatial frequency adaptation: Threshold elevation and perceived contrast. *Vision Research, 36*, 1797–1809.

Solomon, J. A. (2009). The history of dipper functions. *Attention, Perception and Psychophysics, 71*, 435–443.

Stromeyer, C. F., Klein, S., Dawson, B. M., & Spillmann, L. (1982). Low spatial-frequency channels in human vision: Adaptation and masking. *Vision Research, 22*, 225–233.

Sutter, A., Sperling, G., & Chubb, C. (1995). Measuring the spatial frequency selectivity of second-order texture mechanisms. *Vision Research, 35*, 915–924.

Tanaka, H., & Ohzawa, I. (2009). Surround suppression of V1 neurons mediates orientation-based representation of high-order visual features. *Journal of Neurophysiology, 101*, 1444–1462.

Westrick, Z. M., Henry, C. A., & Landy, M. S. (2013). Inconsistent channel bandwidth estimates suggest winner-take-all nonlinearity in second-order vision. *Vision Research, 81*, 58–68.